

Figure S1. Frequency distribution histograms for raw (untransformed), log-transformed, and RIN-transformed FP1 EEG site data for eyes-closed condition ($n = 98$).

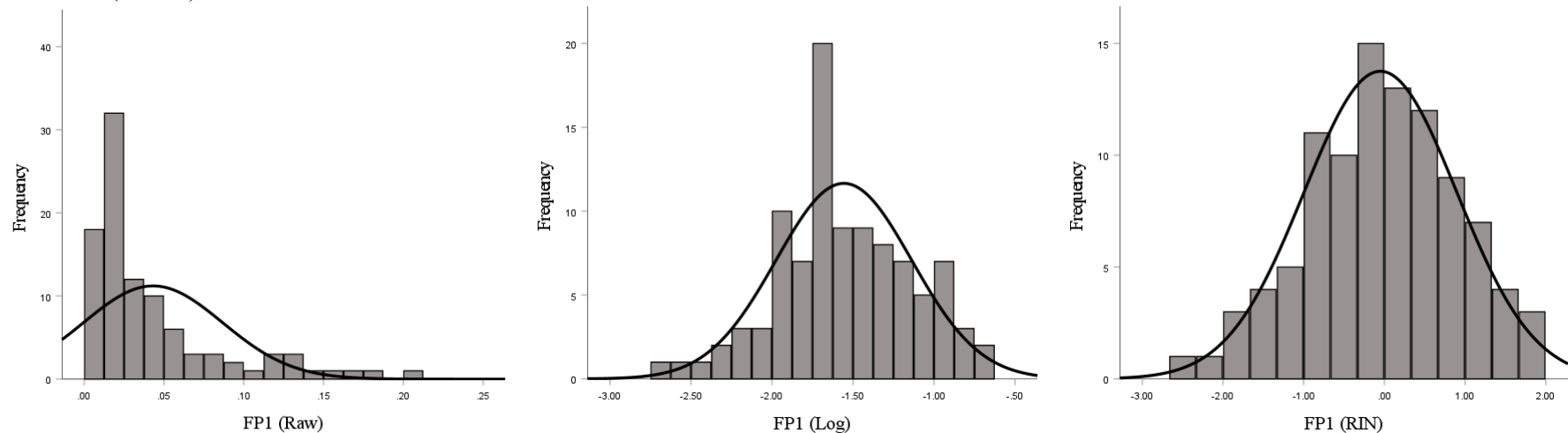


Figure S2. Frequency distribution histograms for raw (untransformed), log-transformed, and RIN-transformed FP2 EEG site data for eyes-closed condition ($n = 98$).

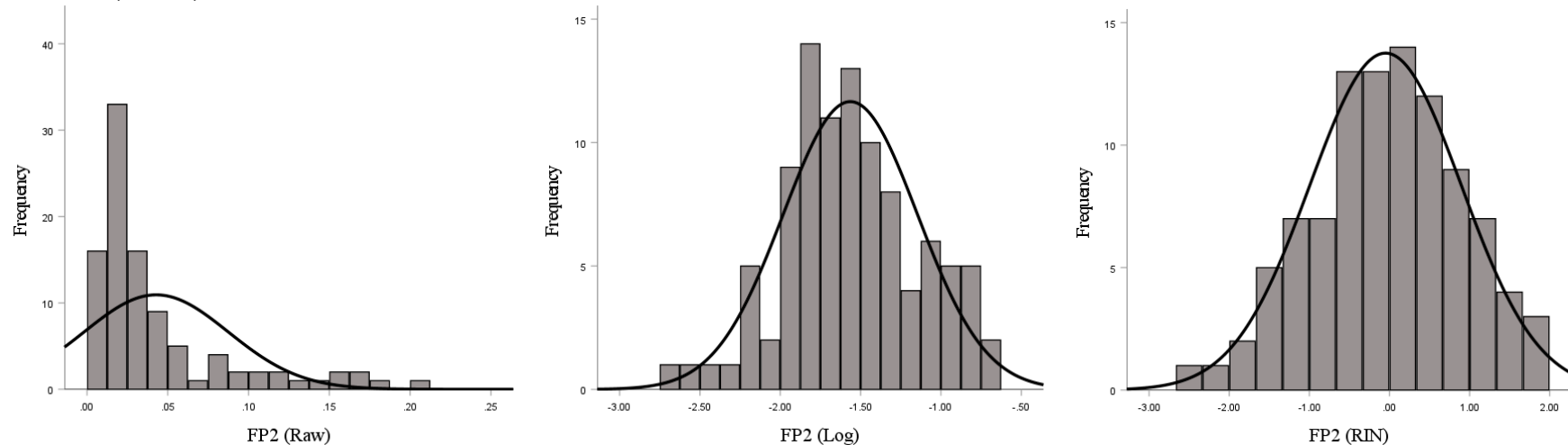


Figure S3. Frequency distribution histograms for raw (untransformed), log-transformed, and RIN-transformed F3 EEG site data for eyes-closed condition ($n = 98$).

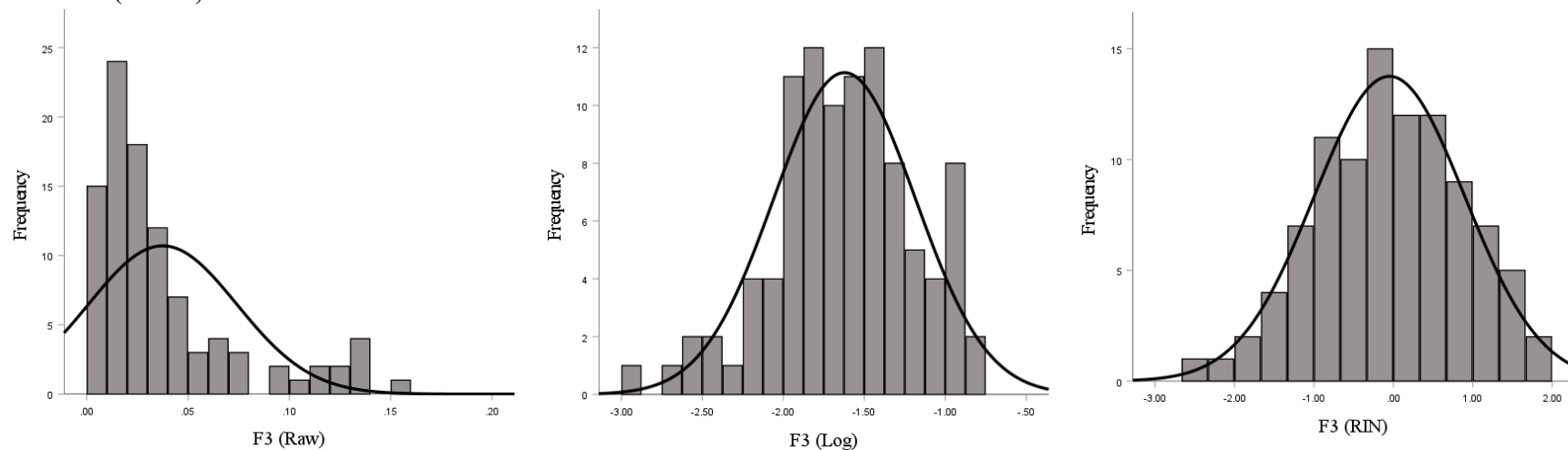


Figure S4. Frequency distribution histograms for raw (untransformed), log-transformed, and RIN-transformed F4 EEG site data for eyes-closed condition ($n = 98$).

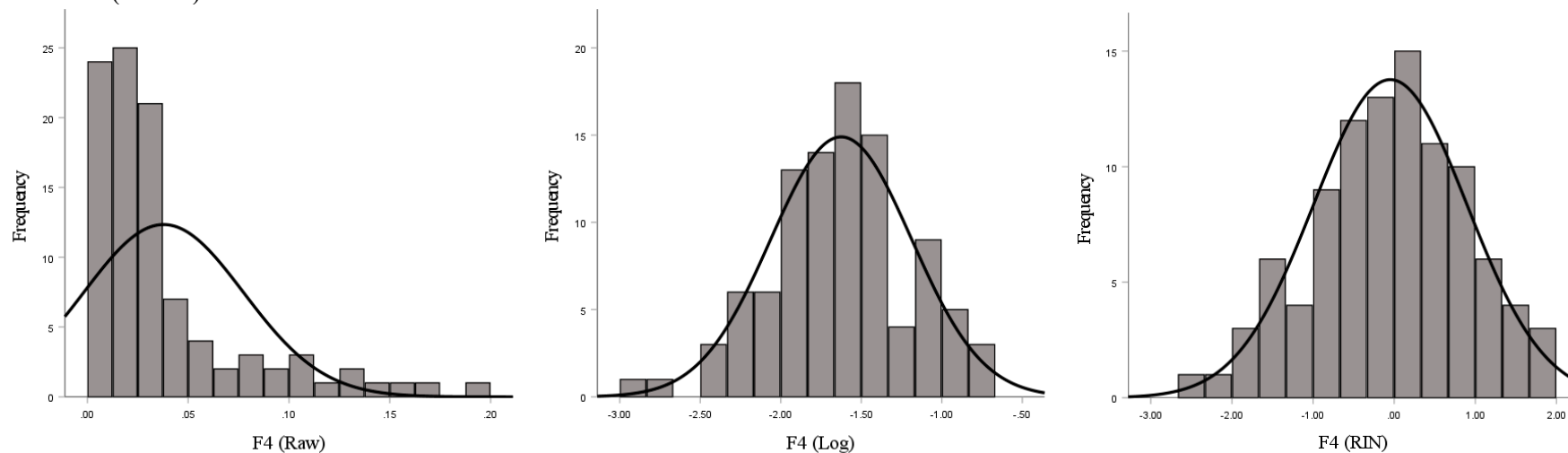


Figure S5. Frequency distribution histograms for raw (untransformed), log-transformed, and RIN-transformed F7 EEG site data for eyes-closed condition ($n = 98$).

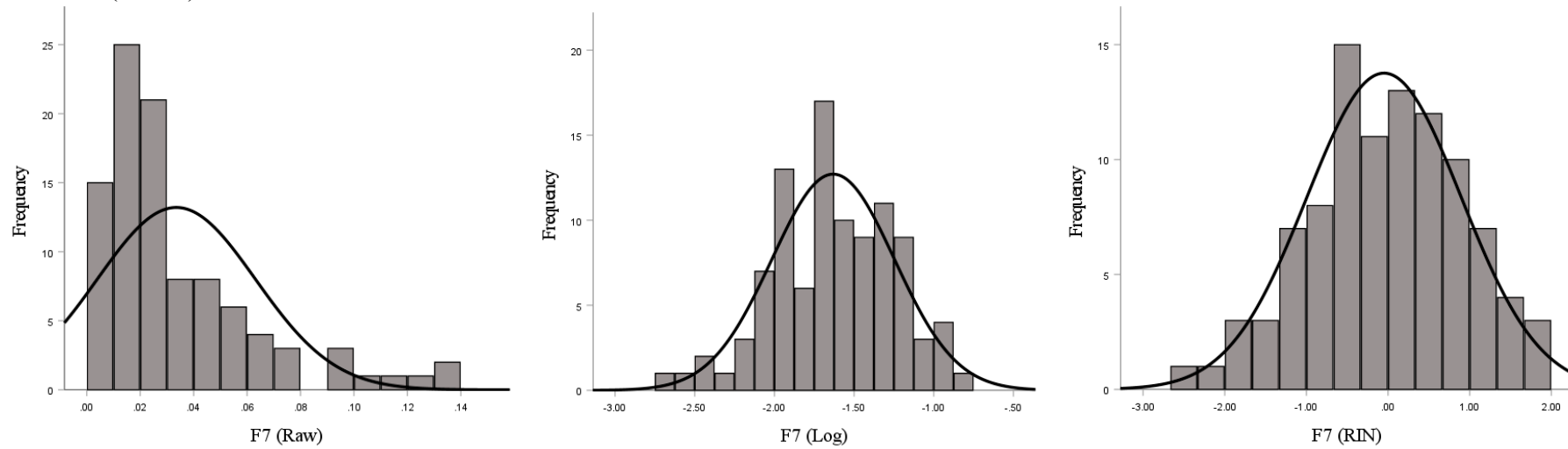


Figure S6. Frequency distribution histograms for raw (untransformed), log-transformed, and RIN-transformed F8 EEG site data for eyes-closed condition ($n = 98$).

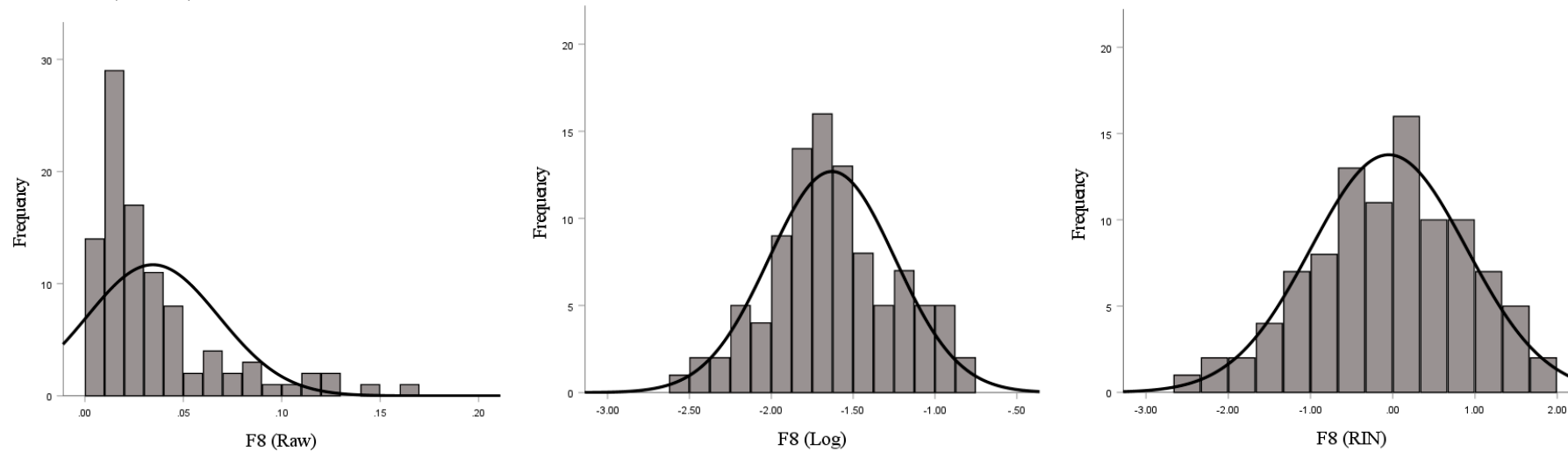


Figure S7. Frequency distribution histograms for raw (untransformed), log-transformed, and RIN-transformed FT7 EEG site data for eyes-closed condition ($n = 98$).

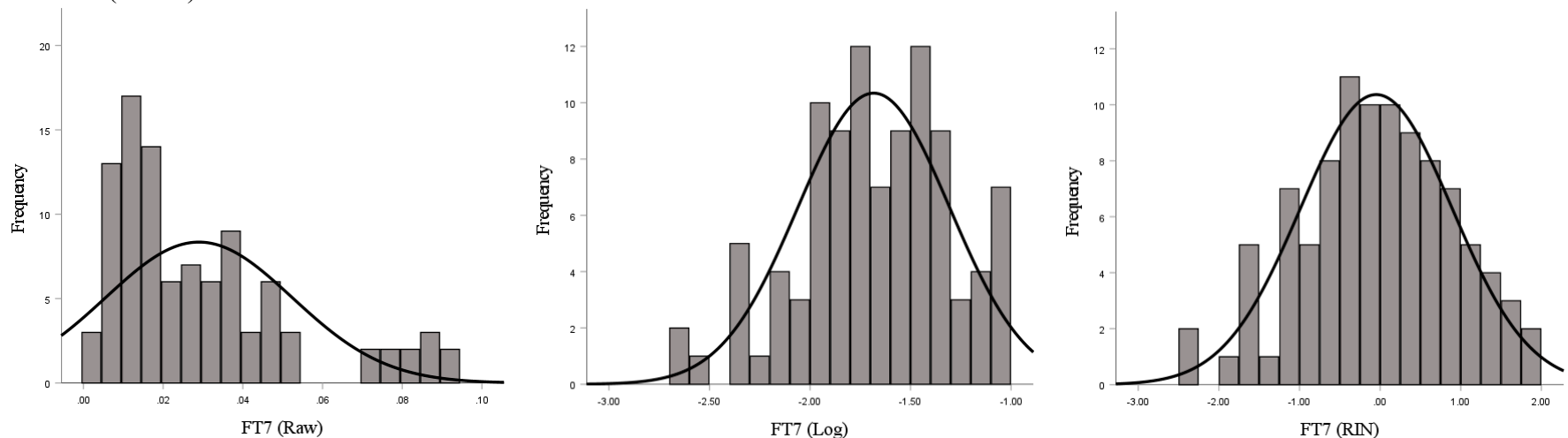


Figure S8. Frequency distribution histograms for raw (untransformed), log-transformed, and RIN-transformed FT8 EEG site data for eyes-closed condition ($n = 98$).

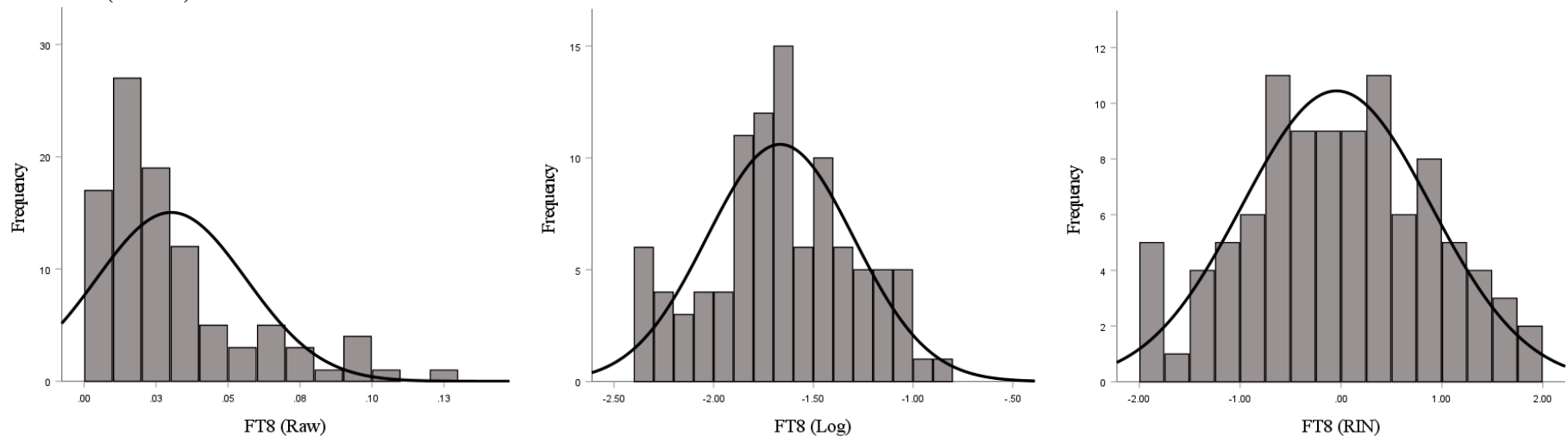


Figure S9. Frequency distribution histograms for raw (untransformed), log-transformed, and RIN-transformed FC3 EEG site data for eyes-closed condition ($n = 98$).

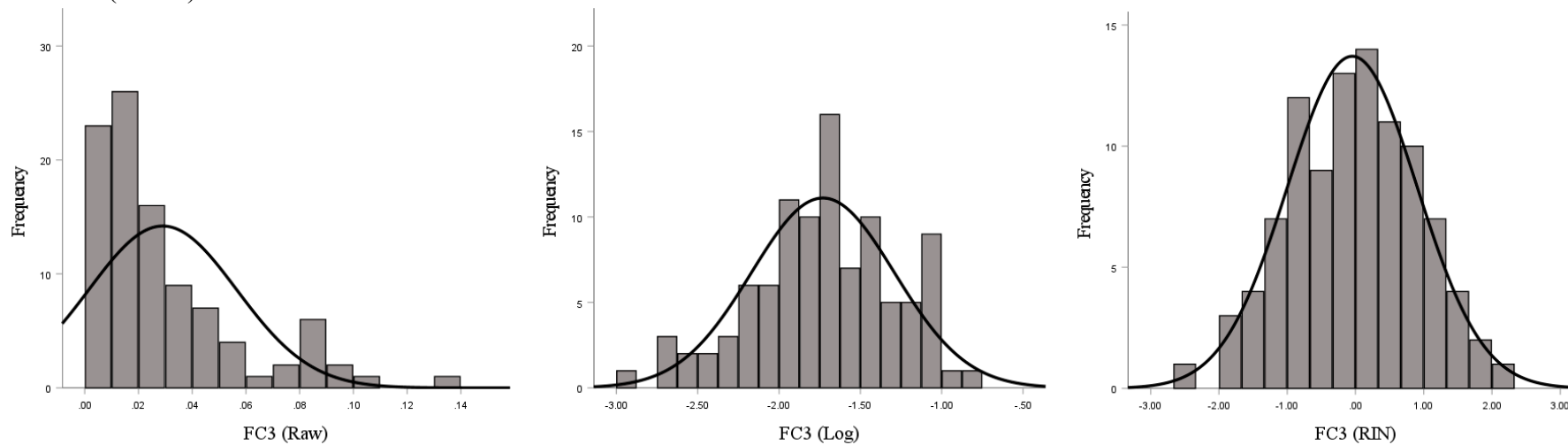


Figure S10. Frequency distribution histograms for raw (untransformed), log-transformed, and RIN-transformed FC4 EEG site data for eyes-closed condition ($n = 98$).

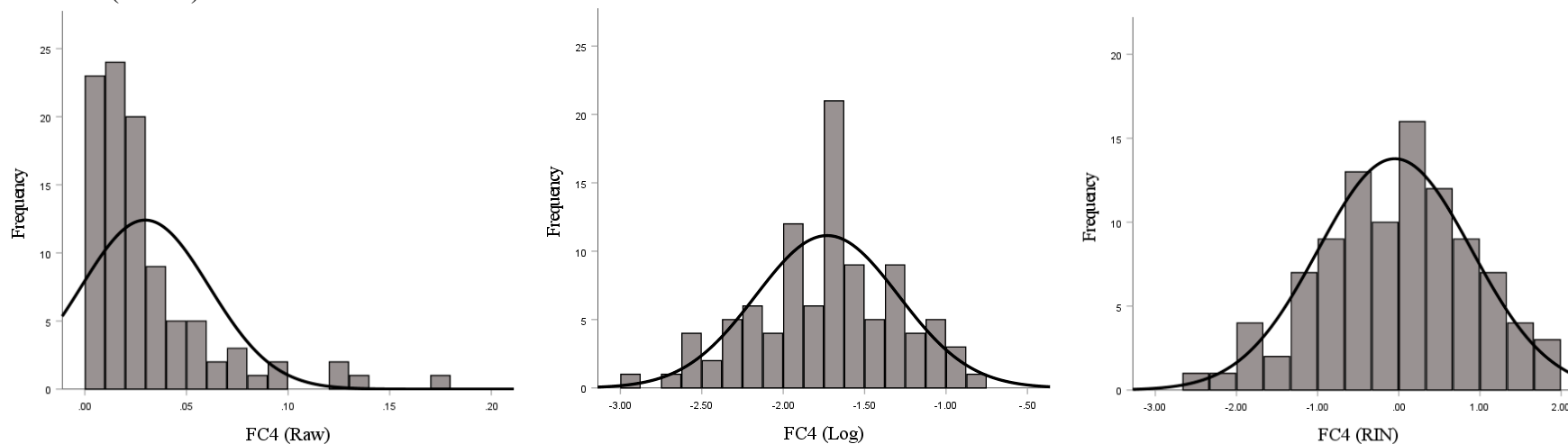


Figure S11. Frequency distribution histograms for raw (untransformed), log-transformed, and RIN-transformed FP1 EEG site data for eyes-open condition ($n = 95$).

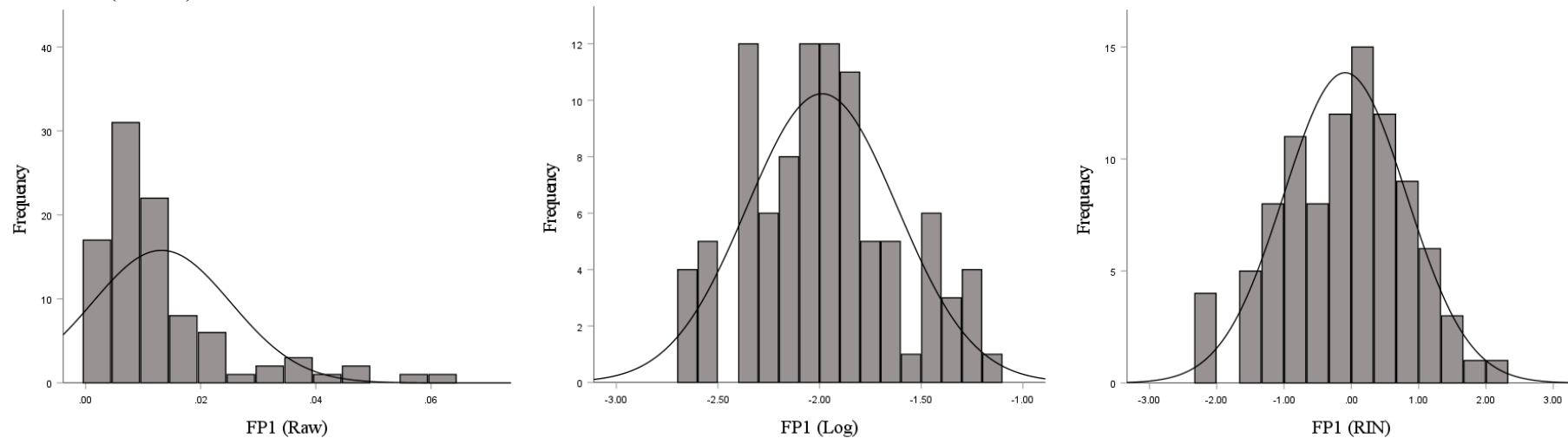


Figure S12. Frequency distribution histograms for raw (untransformed), log-transformed, and RIN-transformed FP2 EEG site data for eyes-open condition ($n = 95$).

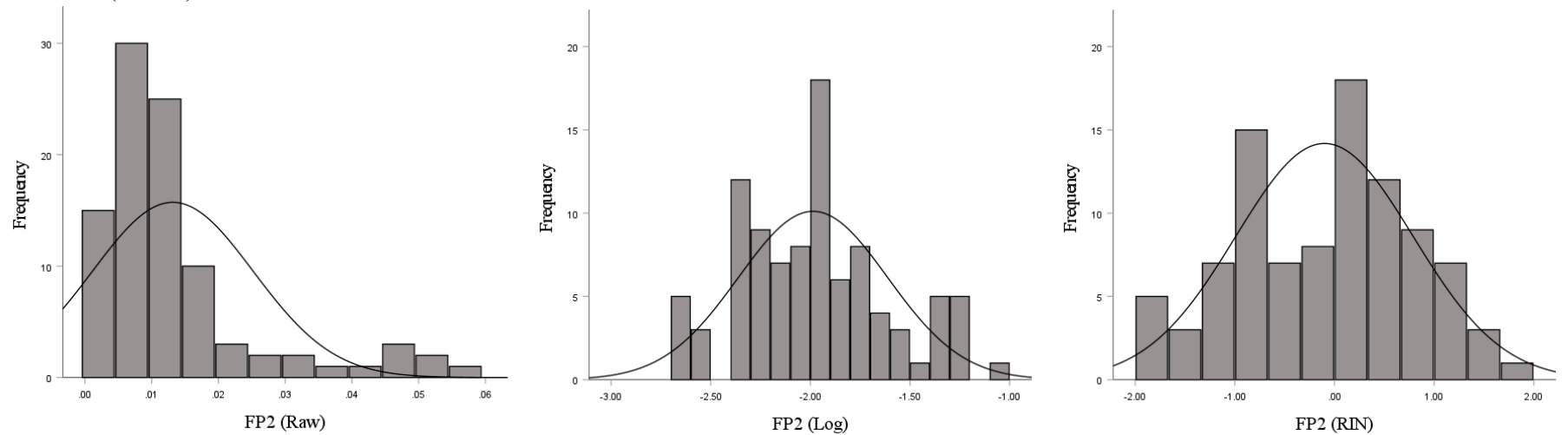


Figure S13. Frequency distribution histograms for raw (untransformed), log-transformed, and RIN-transformed F3 EEG site data for eyes-open condition ($n = 95$).

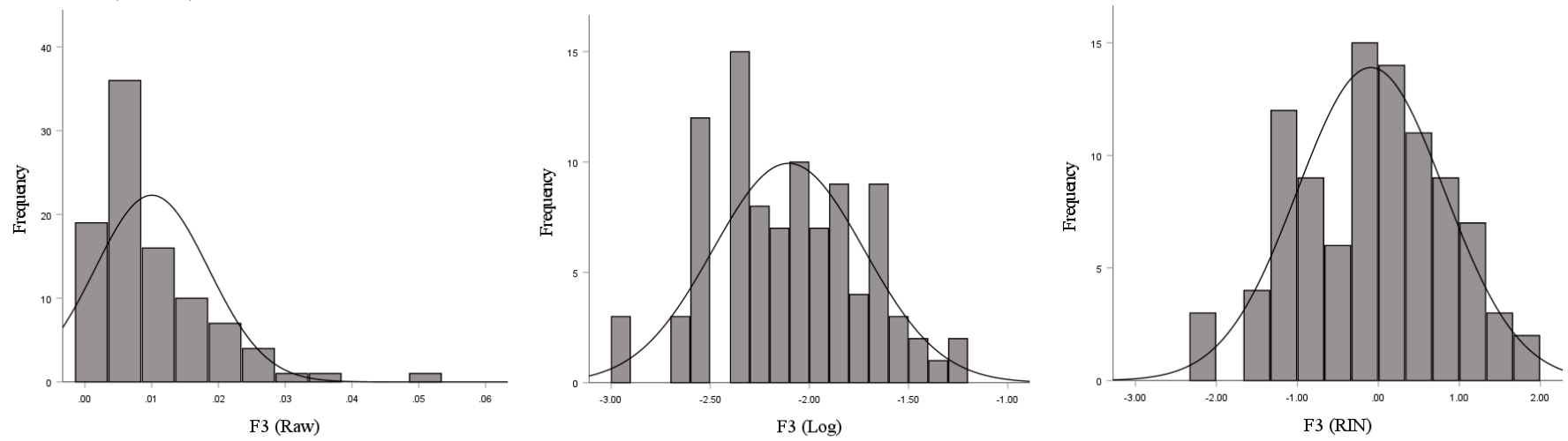


Figure S14. Frequency distribution histograms for raw (untransformed), log-transformed, and RIN-transformed F4 EEG site data for eyes-open condition ($n = 95$).

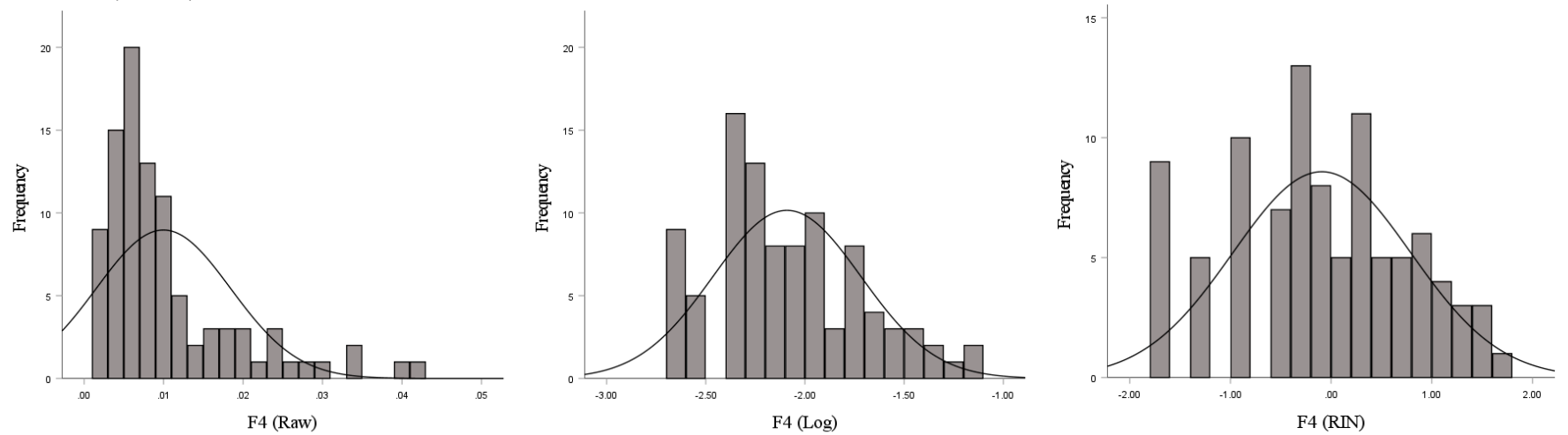


Figure S15. Frequency distribution histograms for raw (untransformed), log-transformed, and RIN-transformed F7 EEG site data for eyes-open condition ($n = 95$).

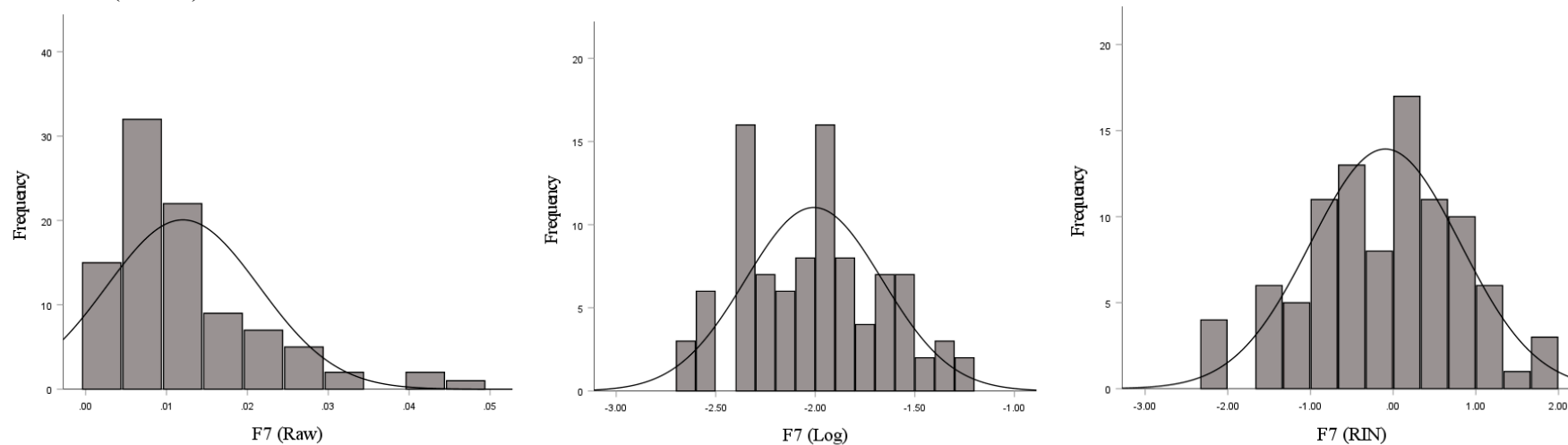


Figure S16. Frequency distribution histograms for raw (untransformed), log-transformed, and RIN-transformed F8 EEG site data for eyes-open condition ($n = 95$).

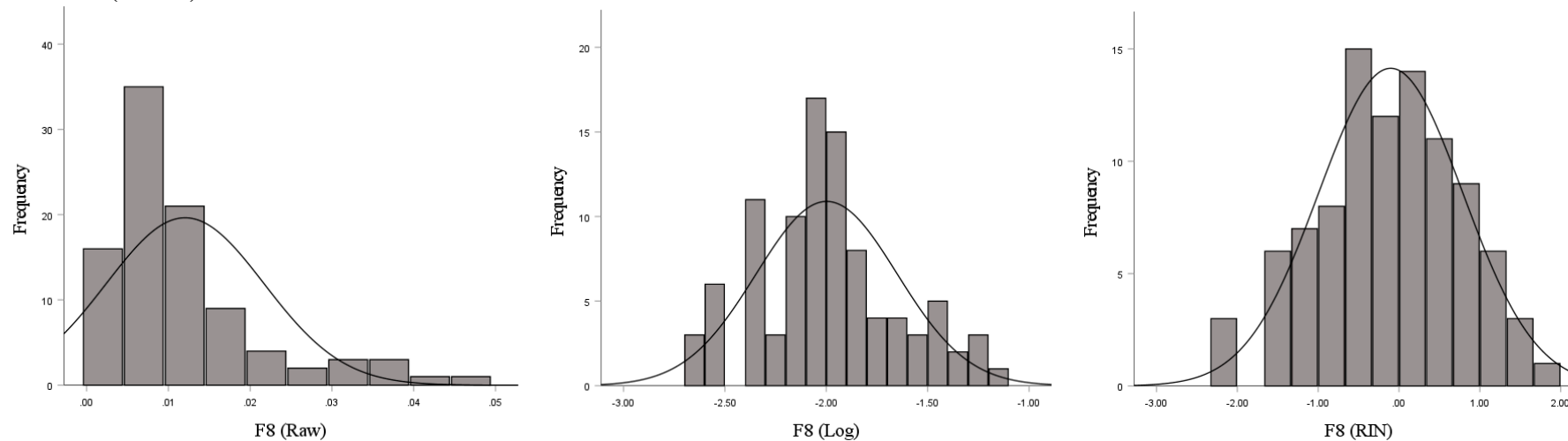


Figure S17. Frequency distribution histograms for raw (untransformed), log-transformed, and RIN-transformed FT7 EEG site data for eyes-open condition ($n = 95$).

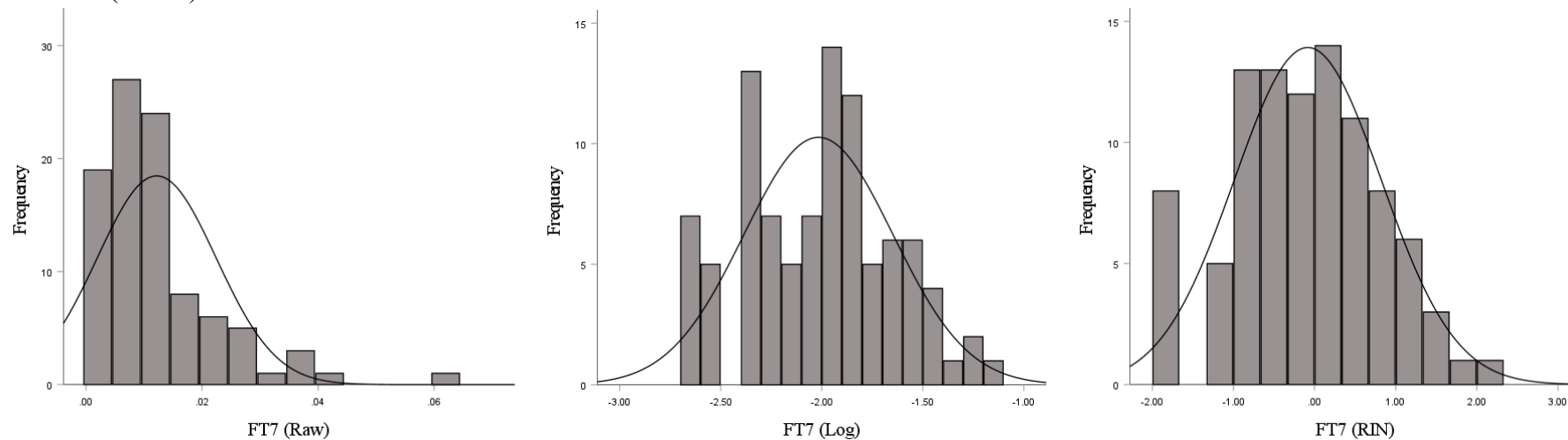


Figure S18. Frequency distribution histograms for raw (untransformed), log-transformed, and RIN-transformed FT8 EEG site data for eyes-open condition ($n = 95$).

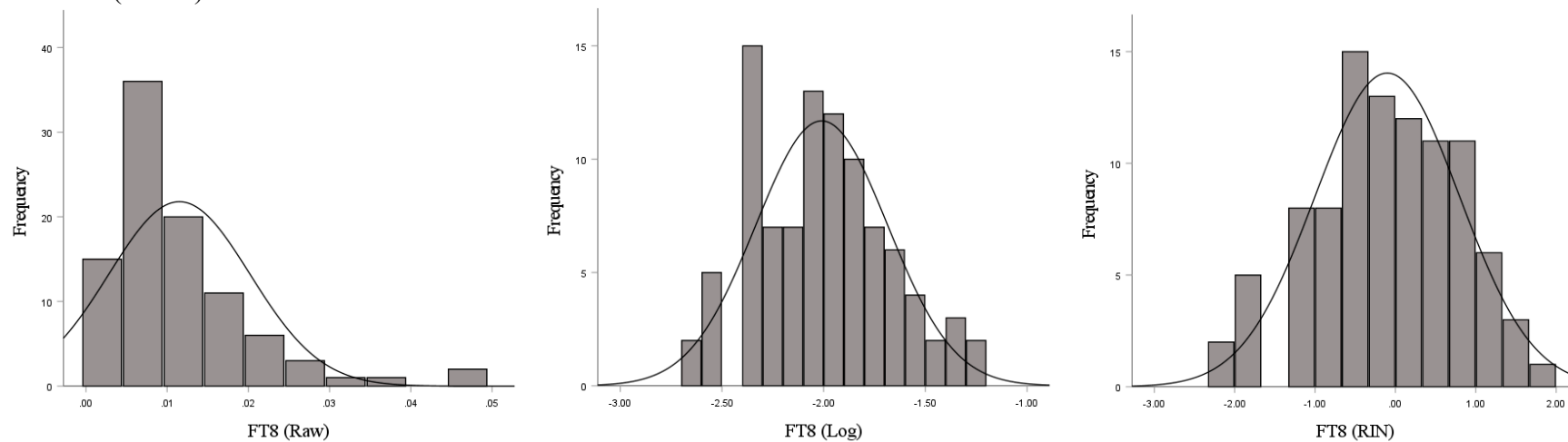


Figure S19. Frequency distribution histograms for raw (untransformed), log-transformed, and RIN-transformed FC3 EEG site data for eyes-open condition ($n = 95$).

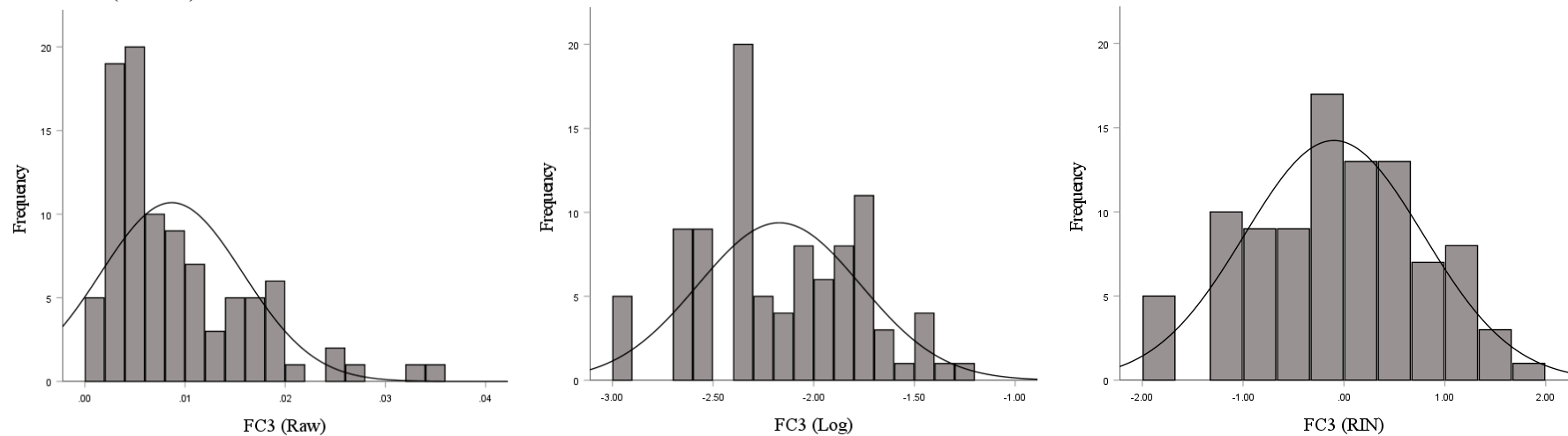


Figure S20. Frequency distribution histograms for raw (untransformed), log-transformed, and RIN-transformed FC4 EEG site data for eyes-open condition ($n = 95$).

